Available online at www.sciencedirect.com

ScienceDirect

Procedia Structural Integrity 3 (2017) 395–401

Structural Integrity Procedia

www.elsevier.com/locate/procedia

XXIV Italian Group of Fracture Conference, 1-3 March 2017, Urbino, Italy

The numerical modelling of a middle strength rock material under Flexural test by Finite Element method-coupled to-SPH

A. Mardalizad[a], A. Manes[a]*, M. Giglio[a].

[a]*Politecnico di Milano, Department of Mechanical Engineering, Via La Masa, Milan 20156, Italy*

Abstract

Proper fracture assessment of the geological materials, which are highly exposed to hydrostatic loading, is a persistent challenge, in particular when aiming to develop an adequate numerical modelling technique. The mechanical response of a middle strength rock, namely Pietra Serena sandstone, under a Flexural (Four-Point Bending) test is investigated numerically in this study. The FEM-coupled to-SPH numerical technique has been approached in conjunction with an advanced material model implemented in LS-DYNA, namely the Karagozian and Case Concrete (KCC) model. The state of stress is investigated in different parts of the specimen in order to determine the strength of the material and the crack initiation area. The numerical results are finally validated by experimental data to show the reliability of the model.

Keywords: Rock; Flexural; ASTM; KCC; FEM; SPH; LS-DYNA

1. Introduction

The purpose of this study is to investigate the mechanical response of a middle strength rock to a Flexural test, also called Four-Points Bending test, by means of an appropriate numerical modelling technique and validation via a standard experimental testing program. Due to several issues, it is inconvenient to determine the maximum principal

* Corresponding author. Tel.: +39-02-2399-8630; fax: +39-02-2399-8263.
E-mail address: andrea.manes@polimi.it

10.1016/j.prostr.2017.04.050

tensile strength of rock materials, which is one of the most significant parameters in the deformability of rocks, by means of the direct tensile test. Therefore, rock engineers are required to design other testing approaches which are capable of indirectly presenting the normal tensile stresses (at least) in a specific portion of the specimen.

The implementation of adequate numerical modelling in conjunction with affordable constitutive models has become an indispensable tool in the stress analysis domain. As far the numerical modelling technique of this study is concerned, it was decided to apply the Finite Element Method (FEM) coupled to Smooth Particle Hydrodynamics (SPH), so that the specimen was first modelled by hexagonal Lagrangian three-dimensional elements. An external algorithm was then implemented to eliminate those elements which reach a specific failure level and subsequently these eroded elements were replaced by SPH particles with exactly the same mechanical properties. This method takes advantage of both the accuracy of the Lagrangian FE (before the occurrence of high distortion) and the ability of the SPH method to cope with large deformation, mesh distortion, etc.

The commercial numerical solver LS-DYNA was implemented due to the existence of a large and adequate library of material models as well as due to the solver's capability to deal with high nonlinear numerical simulations. The Karagozian and Case Concrete (KCC) model was employed in this study. It is an advanced material model which consists of three fixed independent failure levels. This material model decouples the volumetric and deviatoric responses and also analyses the accumulated damage of the elements. The comparison of the numerical and experimental results was critically discussed in order to show the precision of this study.

Nomenclature

σ_{fl}	flexural strength, [MPa]
W	maximum load [N]
L	span length of the specimen
b	width of the specimen
d	depth of specimen
a	further nomenclature continues down the page inside the text box
f'_c	unconfined compressive strength
f_t	tensile strength
ψ	empirical strength index of a brittle material

2. Experimental test arrangement

The experimental configuration for the Flexural test, suggested by the ASTM standard (ASTM, 1998), consists of a rectangular cubic specimen which is supported by two fixed rollers near the end of its length span and loaded vertically by means of two compressive rollers at a certain distance from the center of the specimen (see Fig. 1. a). This symmetrical configuration causes nominally zero shear forces between the two compressive rollers, and accordingly constant bending moment at this area. The normal compressive and tensile stresses act at the top and bottom of this middle span, respectively. The maximum principal stress, which corresponds to the ultimate loading value, according to the beam theory, can be determined. This maximum stress is called the flexural strength and gives a rough approximation about the principal tensile strength. However, the flexural strength tends to overestimate the tensile strength due to some issues, i.e. the estimation process considers a linear relationship as the stress-strain behaviour of the material at its critical cross-section and furthermore all the materials have a certain amount of anisotropic level in their structure (Biolzi, Cattaneo, & Rosati, 2001). Therefore, the flexural strength σ_{fl} [MPa], which is given by the equation (1), can be considered as a parameter to validate the numerical models.

$$\sigma_{fl} = \frac{3WL}{4bd^2} \tag{1}$$

The experimental tests within this research work were conducted on three rectangular cubic specimens of Pietra Serena sandstone with the same geometries. The span length L, width b and depth d of all the specimens are equal to 318, 102 and 32 [*mm*], respectively. However, the total length of the specimen is measured as 381 [*mm*]

As can be seen in Fig. 1, two pairs of steel rods are embedded to the testing apparatus. The center of lower rods are fixed to the bed of testing machine while the upper rods are displacement controlled by means of a compressive platen. According to (ASTM, 1998) the speed is set to 0.2 mm/min in order to apply the load at a uniform stress rate of 4.14 MPa.

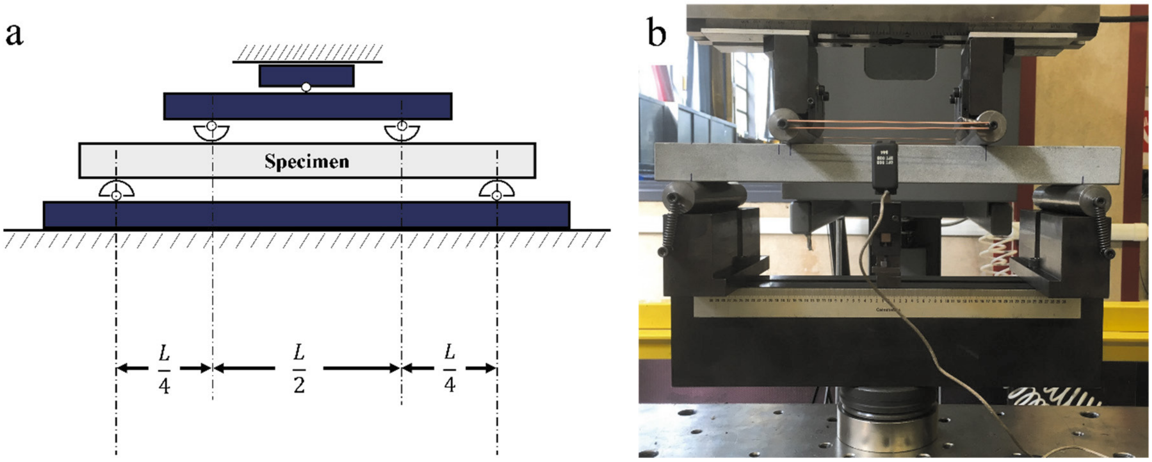

Fig. 1. (a) ASTM arrangement of Flexural test (ASTM, 1998); (b) corresponding experimental layout of this research work

Fig. 2 indicates two of the specimens after the flexural tests. The crack initiates at the lower part, which is subjected to tension stresses, in all of the specimens and then propagates in an upward manner through the depth. Also, the cracks are located under (and close to) the section of the specimens which were in contact with the moving rods.

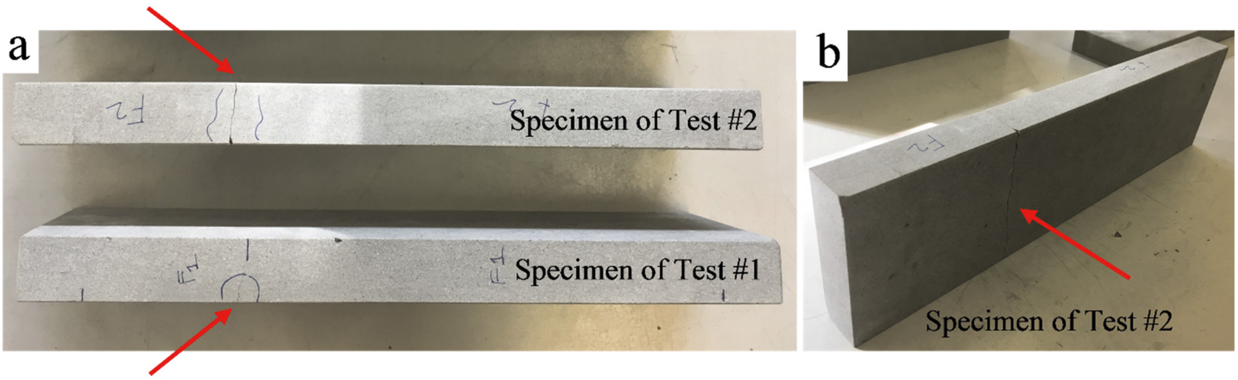

Fig. 2. The broken specimens of Test #1 and Test #2 after performing the flexural test; (a) front view; (b) isometric view

3. Numerical simulation

Among several numerical techniques developed for solid materials in continuum mechanics, the non-linear lagrangian Finite Element Method (FEM) has its own privileges. This is mainly due to its accuracy and the convenient consuming time. One of the main drawbacks of this method, however, is its inability to deal with highly distorted elements. High distortion is quite commonly observed in the post failure behaviour of rocks. Generally speaking, it is inevitable to investigate the fractured rock by FEM without considering the elements that bear severe distortion. It is possible to avoid this drawback of the Lagrangian FEM elements by replacing the severely distorted elements with Smooth Particle Hydrodynamics (SPH) particles after a certain limit. The severe element distortion is avoided in SPH since the nodal connectivity is not fixed. However, generally SPH is less accurate than FEM, but much more inconvenient in terms of computation costs. In order to take advantage of both the FEM and the SPH particles, the innovative method FEM-coupled to-SPH was implemented so that the Lagrangian FEM elements are converted to SPH particles after reaching a certain criterion, while all the mechanical properties, i.e. mass, kinematic variables and constitutive properties remain the same. The development of this numerical technique is expected to be one of the most significant approaches in the rock fracture domain.

In LS-DYNA this method is defined by the keyword ADAPTIVE_SOLID_TO_SPH in which two of its parameters, called ICPL and IOPT, are set to unit. Due to the unavailability of an eroding algorithm in most of the material keywords available in the LS-DYNA library, including the one used in this research, an external erosion algorithm has to be implemented. Therefore, the MAD_ADD_EROSION keyword was utilized in the numerical models of this study. Among all of the fields of this keyword which can be used to define the proper criteria for the deletion of the elements, the maximum principal strain (MXEPS) was selected here. Hence 1, 8 or 27 SPH particles can be defined for each eroded hexagonal element, while, in order to keep the time consumption cost low in this study, each element can be converted only to one SPH particle.

Replication of the Flexural test was therefore obtained by means of a numerical model that consist of five parts including two rollers, two compressive platens and the specimen. Due to the symmetric nature of the test, only one-quarter of the test was modelled. All of these parts, except the rock specimen, were considered simply as rigid bodies. Therefore, the conversion to SPH particles can be defined only for the specimen. The axes of both rollers were fixed in the XY plane, while the displacement-controlled compressive loading was applied by the upper platen. The lower platen was limited to zero degree of freedom to represent the bed of the testing machine.

The numerical modelling of rock specimen was obtained by implementing an advanced hydrostatic pressure-dependent material model, called Karagozian and Case Concrete (KCC or K&C) model, developed by Malvar et al. within 1995 to 1997 (L. Malvar, Crawford, Wesevich, & Simons, 1996; L. J. Malvar, Crawford, & Morrill, 2000; L. J. Malvar, Crawford, & Wesevich, 1995; L. J. Malvar, Crawford, Wesevich, & Simons, 1997). It consists of three independent fixed failure surfaces; yield $\Delta\sigma_y$, maximum $\Delta\sigma_m$ and residual $\Delta\sigma_r$

(see Fig. 3.a), and a linear interpolation function is used in order to consider the damage accumulation based on the current state of stress. The three-dimensional stress space of this model and the three failure surfaces are expressed in Fig. 3.c. The effect of Lode angle is considered within the KCC model as can be seen in the deviatoric plane (see Fig. 3.b). The comprehensive definition of this model is explained in details at (L. J. Malvar, et al., 1997).

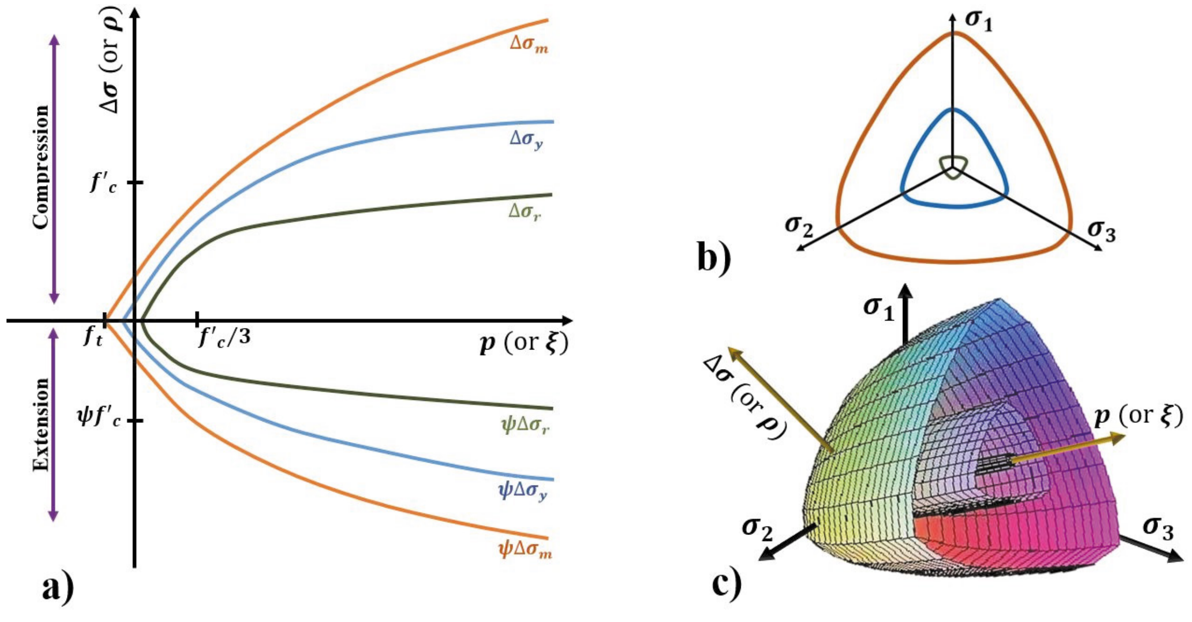

Fig. 3. Failure surfaces of the KCC model in; (a) compression/tension meridian; (b) deviatoric plane; and (c) 3D stress space (Brannon & Leelavanichkul, 2009)

The volumetric and deviatoric responses are decoupled by means of an Equation-of-State (EOS) that gives the current pressure as a function of current and previous most compressive volumetric strain. The required EOS keyword which works in conjunction with KCC model in LS-DYNA is called EOS_TABULATED_COMPACTION. Up to ten pairs of pressure-volumetric tabular data can be put in this EOS to describe precisely the rock compaction behaviour. The calibration procedure requires also twenty-two input parameters in the full input version mode. In the meantime another set of independent tables, which is attributed to the damage evaluation parameters (λ) corresponding to the current failure surface (η), needs to be defined (Hallquist, 2014).

The KCC material model is developed in LS-DYNA by MAT_CONCRETE_DAMAGE_R3 (or MAT_072R3). There is a significant user enhancement presented in the third release of this keyword. It provides an automatic input parameter generation opportunity based only on a few parameters, i.e. the unconfined compressive strength. The KCC model has been originally developed to simulate the response of concrete, and although the response of sandstone is expected to be similar to concrete, the automatic input mode results are only a rough estimation for sandstones. However, this automatic method was used initially within this study due to the overwhelming number of input parameters which are difficult to obtain from current resources. Apart from the numerical results which are obtained directly from the automatic mode, LS-DYNA further automatically generates all the input parameters and writes them into the "MESSAG" file. Therefore, some of these parameters (i.e. the damage parameters) can be used in addition to the other parameters provided for the users by other resources. The authors of this research work were unable to find any experimental data about the Pietra Serena sandstone. It was shown within previous studies in (Mardalizad, Manes, & Giglio, 2016, 2017) that the mechanical behaviour of Berea sandstone is expected to be very similar to the Pietra Serena. Therefore, the experimental data in all the models are related to the Berea sandstone. The initial input parameters used for the automatic mode are obtained from (ASTM, 2004) and reported in Table 1.

Table 1. The experimental data of Berea sandstone provided for the automatic mode

RO [ton/mm^3]	PR	A0 [MPa]	NOUT	RSIZE	UCF
2.00e-9	0.34	-62.00	2.00	0.03937	145.00

Where RO and PR are the density and Poisson's ratio, respectively. The parameters RSIZE and UCF are unit conversion factors and the NOUT is called the "output selector for effective plastic strain". It is worth mentioning that in order to define the unconfined compressive strength only at the automatic mode of MAT_072R3 keyword, the A0 should be defined as a negative value. After performing the initial simulation, some of the generated input parameters (i.e. B1, B2, B3, OMEGA, SLambda and LocWidth) and almost all of the EOS tabular data were used for the full input calibration mode. Only the "Pressure02" parameter from EOS keyword was changed to 26.1 [MPa] to reach the same bulk modulus (and accordingly elastic behavior) as the Berea sandstone. The details can be found in (Mardalizad, et al., 2016). The tensile strength parameter was investigated by another recent study of the authors (Mardalizad, et al., 2017) where the Brazilian tensile test was performed on Pietra Serena and the tensile strength was determined as 5.81 [MPa]. The input parameters corresponding to the damage function, indicated by the set of $\eta - \lambda$ data, were changed to what is reported in (Markovich, Kochavi, & Ben-Dor, 2011). One of the most important steps for the calibrating of the KCC model is related to the a_i parameters which can be calibrated by means of the least square curve fitting method from the experimental triaxial compression tests (Jaime, 2011). The experimental data of triaxial compression test performed at four different confining pressures are provided at (Ding, 2013). The a_i parameters, computed based on these experimental data, are reported in Table 2 (the A0 is a positive value).

Table 2. The a_i parameters experimental of Berea sandstone provided for the full input mode

A0 [MPa]	A1 [MPa]	A2	A0Y [MPa]	A1Y [MPa]	A2Y	A1F [MPa]	A2F
34.458	0.65629	0.00097	21.621	1.11569	0.00251	0.7563	0.00097

The hexagonal constant stress solid elements, with ELFORM=1 formulation, were utilized for all the parts. The section of the SPH and the shell elements were set as the default of LS-DYNA as well. The automatic penalty based contact keywords, AUTOMATIC_SURFACE_TO_SURFACE and AUTOMATIC_NODES_TO_SURFACE were applied for solid-solid/shell and SPH-solid contacts, respectively. The static friction coefficient was set to 0.4 and the IGNORE=2 at CONTROL_CONTACT was used to allow the initial penetration. Instead of applying single point constraints to the SPH particles, which can lead to inaccurate results and numerical instabilities, specific boundary conditions at the symmetry planes were imposed (Hallquist, 2014). The BOUNDARY_SPH_SYMMETRY_PLANE keyword creates automatically an imaginary plane which reflects the forces of a set of ghost particles on to the particles in the model. Although these ghost particles have identical properties (i.e. mass, pressure and velocity) as the real ones, they do not physically exist and simply contribute to the particle approximation (Anghileri, Castelletti, Francesconi, Milanese, & Pittofrati, 2011). The maximum principal strain (MXEPS), which is considered as the eroding criteria for FEM to SPH particles conversion should be defined as the final step for the numerical simulation. For this purpose, first the simulation should be run without the MAD_ADD_EROSION implementation to examine the presence of highly distorted elements and to identify the MXEPS at that time step. Within this study, the MXEPS was set to 0.04. The distribution of numerical stress solutions at failure and the crack propagation patterns are shown in Fig. 4.

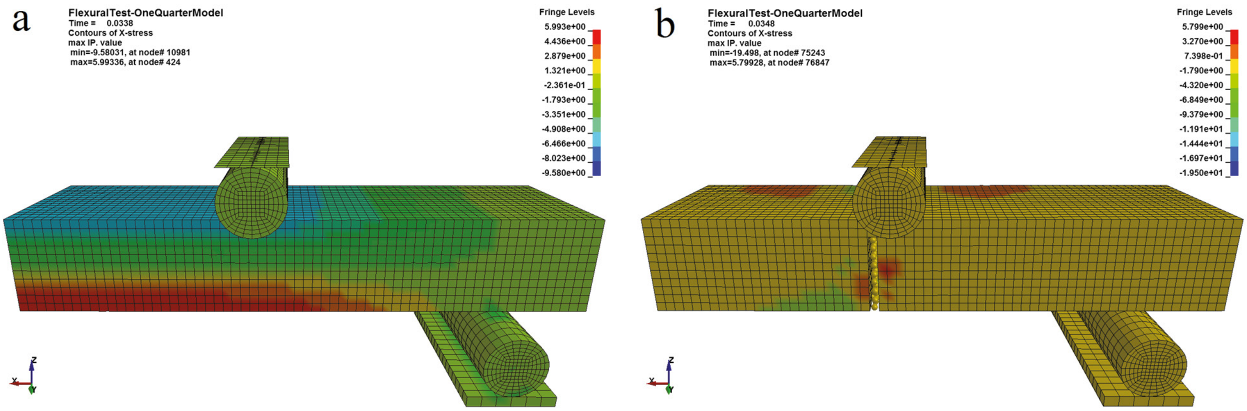

Fig. 4. Distribution of numerical stresses in the X direction (along length); (a) the maximum value before failure; (b) after failure.

The Fig. 4. (a) represents the distribution of the X stress (along the length of specimen) one time step before failure. As can be seen the tensile and the compressive stresses are present in the element below and above the neutral axis, respectively.

4. Comparison of numerical simulation result and experimental data

The flexural strengths of three experimental tests as well as the corresponding values from the numerical models are reported in Table 3. The numerical results obtained by the automatic input generation of the KCC model underestimated the average experimental results by an error of about 24%, while this drawback is significantly improved for the manual calibrated material model. Due to the fact that in the full input mode of KCC all the parameters are defined based on the Berea sandstone, i.e. the triaxial compression experimental data, and also the spread of the experimental results, the numerical results seem reliable. It is worth mentioning that the unconfined compressive strength, which greatly influences the numerical results, is considered as 62 [MPa] within this study. However, it is not possible to impose a precise value for this parameter since many issues may affect it, in particular the humidity. The other numerical simulations obtained by simply increasing this parameter eventuated closer values to the average of experimental flexural strength, while they are not reported here due to the consistency of the input parameter resource.

Table 3. The flexural strength of Pietra Serena sandstone

	Test #1	Test #2	Test #3	**KCC Automatic**	**KCC Manual Calibration**
flexural strength σ_{fl} [MPa]	8.3124	10.024	9.7927	**7.1104**	**8.1216**
Average of experimental results [MPa]				**9.3764**	

The crack propagation pattern as shown in Fig. 4. (b), captured at some time steps after failure. The comparison of this Fig. 4 and Fig. 2 shows that the numerical simulation precisely replicates the experimental crack pattern, which is located under the section in contact with the moving rods.

5. Conclusion

The numerical modelling of the Flexural (four-point bending) test has been successfully developed and compared to the experimental data. All the experimental tests were performed based on the protocols of the ASTM standard. The Karagozian and Case Concrete model shows a significant enhancement when the material input parameters are calibrated and directly inserted into the material keyword, instead of the automatic input generator mode. The numerical results are still expected to be improved by a direct material identification based on the Pietra Serena, i.e. a triaxial compression test. However, the numerical simulations provided within this study prove the functionality and reliability of KCC material model in the replication of the Flexural test.

References

Anghileri, M., Castelletti, L.-M. L., Francesconi, E., Milanese, A., Pittofrati, M. (2011). Rigid body water impact–experimental tests and numerical simulations using the SPH method. International Journal of Impact Engineering, 38, 141-151.

ASTM. (1998). Test Method for Flexural Strength of Dimension Stone. In C 880-98. West Conshohocken, PA: ASTM International.

ASTM. (2004). Standard Test Method for Compressive Strength and Elastic Moduli of Intact Rock Core Specimens under Varying States of Stress and Temperatures. In D 7012-04. West Conshohocken, PA: ASTM International.

Biolzi, L., Cattaneo, S., Rosati, G. (2001). Flexural/tensile strength ratio in rock-like materials. Rock mechanics and rock engineering, 34, 217-233.

Brannon, R. M., Leelavanichkul, S. (2009). Survey of four damage models for concrete. Sandia Laboratories, Albuquerque. Sandia Report No. SAND, 5544.

Ding, J. (2013). Experimental Study on Rock Deformation and Permeability Variation. Texas A&M University.

Hallquist, J. O. (2014). LS-DYNA® Keyword User's Manual: Volumes I, II, and III LSDYNA R7. 1. Livermore Software Technology Corporation, Livermore (LSTC), Livermore, California, 1265.

Jaime, M. C. (2011). Numerical modeling of rock cutting and its associated fragmentation process using the finite element method. University of Pittsburgh.

Malvar, L., Crawford, J., Wesevich, J., Simons, D. (1996). A new concrete material model for DYNA3D-Release II: shear dilation and directional rate enhancements. A Report to Defense Nuclear Agency under Contract No. DNA001-91-C-0059.

Malvar, L. J., Crawford, J. E., Morrill, K. B. (2000). K&C concrete material model release III-automated generation of material model input. K&C Technical Report TR-99-24-B1.

Malvar, L. J., Crawford, J. E., Wesevich, J. W. (1995). A Concrete Material Model for DYNA3D. Proceedings of the 10th ASCE Engineering Mechanics Conference.

Malvar, L. J., Crawford, J. E., Wesevich, J. W., & Simons, D. (1997). A plasticity concrete material model for DYNA3D. International Journal of Impact Engineering, 19, 847-873.

Mardalizad, A., Manes, A., Giglio, M. (2016). An investigation in constitutive models for damage simulation of rock material. In AIAS – Associazione Italiana Per L'analisi Delle Sollecitazioni. Trieste, Italy.

Mardalizad, A., Manes, A., Giglio, M. (2017). Investigating the tensile fracture behavior of a middle strength rock: experimental tests and numerical models. In 14th International Conference on Fracture (ICF14). Rhodes, Greece.

Markovich, N., Kochavi, E., Ben-Dor, G. (2011). An improved calibration of the concrete damage model. Finite Elements in Analysis and Design, 47, 1280-1290.